Convergence Analysis for Initial Condition Estimation in Coupled Map Lattice Systems

Lanxin Lin, Minfen Shen, H. C. So and C. Q. Chang

Abstract

In this paper, we focus on studying the problem of initial condition estimation for chaotic signals within the coupled map lattice (CML) systems. To investigate the effectiveness of a CML initial condition estimation method with different maps and coupling coefficients, the convergence and divergence properties of the inverse CML systems are analyzed. Inverse largest Lyapunov exponent (ILLE) is proposed to investigate the strength of convergence and divergence in the inverse CML systems, and it can determine if the CML initial condition estimation method is effective. Computer simulations are included to verify the relationship between the effectiveness of the CML initial condition estimation method and its corresponding ILLE.

Index Terms

Coupled map lattice; Symbolic dynamic; Initial condition estimation; Largest Lyapunov exponent; Signal processing.

I. Introduction

Many research works indicate that chaos is the most common phenomenon in the nature [1]. Being a kind of deterministic signals, chaos draws great attention for its characteristics of internal randomness, meaning that chaotic signals are deterministic but their behavior appears to be random [2]. In the presence of additive disturbance, we can extract the deterministic chaos from the random noise by using the initial condition, if the dynamic of the system is known *a priori* [3]–[7]. As a result, the problem of initial condition estimation of chaotic signals is an important research topic.

For one-dimensional (1-D) temporal chaotic map, it has been proved in [6] that there is a one-to-one correspondence between the set of global orbits in the 1-D temporal chaotic dynamical system and the set

Lanxin Lin and H. C. So are with Department of Electronic Engineering, City University of Hong Kong, Hong Kong, China; Minfen Shen is with Department of Electronic Engineering, Shantou University, Shantou, Guangdong, China; C. Q. Chang is with Department of Electrical and Electronic Engineering, The University of Hong Kong, Hong Kong SAR, China

of its corresponding admissible symbolic sequence. An 1-D temporal initial condition estimation method based on the symbolic dynamics has been proposed in [7]. This method first symbolizes the chaotic signal in the presence of noise, and then estimates the initial condition from the symbolic sequence. This symbolic dynamics based method is effective for 1-D temporal chaotic signals, and its estimation error converges exponentially with its Lyapunov exponent [7].

However, there exist many spatiotemporal chaotic signals in real physical systems in fields as diverse as communication, chemistry, biology, engineering and ecology [8], [9]. Coupled map lattice (CML), which reproduces the essential features of spatiotemporal phenomena, has been of great interest in the chaos research [10]. Knowing the initial condition can facilitate the analysis of the internal dynamics of the spatiotemporal signals. Moreover, the sea clutter, radar echoes from a sea surface, is a spatiotemporal signal and can be modeled by CML system [11]. When the initial condition is effectively estimated, we are able to reconstruct the noise-free chaotic signals, indicating that more robust detectors [11] for them can be devised. In order to estimate initial condition in CML systems, the first idea is to simplify the CML into a temporal chaotic map without considering the effect of spatial coupling [12]. An improvement using time-varying temporal chaotic map model has been proposed [13] to recover the initial condition when the coupling is very weak in CML systems. Since [12], [13] are mainly based on the idea of temporal initial condition estimation, they can only imprecisely recover the initial condition from the weak coupled CML systems, and the estimation errors may be unacceptable for strongly coupled chaotic systems. Consequently, it is necessary to investigate a more accurate method to estimate initial condition in CML systems.

The relationship between symbolic dynamics and CML dynamical system has been investigated in [14]. It is proved that the symbolic description is a complete and effective representation for studying pattern formation in CML systems. Based on this work, a CML initial condition estimation method is proposed in [8], [15] by introducing its symbolic dynamic and it is proved that any point in the state space will converge to its initial condition with respect to sufficient backward iterations when the inverse function of the CML is a contraction map. As a matter of fact, the contraction mapping theorem only provides a sufficient condition of convergence [16], [17]. This means that contraction map just produces one of the sufficient conditions to support the existence of a fixed point that leads to the convergence. In [16], [17], we have proved that the inverse function of a CML system with logistic map is not a contraction map even when the coupling coefficient is significant small. We also claim that this CML initial condition estimation method still works when the inverse system is fully convergent. That is to say, the convergence strength is larger than its divergence strength in backward iterative procedure. However, there is still no investigation on measuring the convergence and divergence strength. In this work, we further study the convergence and divergence properties of inverse CML systems and then provide the necessary and sufficient condition for effective initial condition estimation.

The rest of this paper is organized as follows. The background and technique of the initial condition estimation problem based on symbolic dynamics are presented in Section II. In Section III, the convergence and divergence properties of inverse CML systems with different maps and coupling coefficients are investigated by the inverse largest Lyapunov exponent (ILLE). The necessary and sufficient condition for effective initial condition estimation is also given. The Cramér-Rao lower bound (CRLB) of the estimated initial conditions in uncorrelated Gaussian noise is derived in Section IV. Simulation results are included in Section V to confirm the proposed necessary and sufficient condition. Finally, conclusions are drawn in Section VI.

II. CML Initial Condition Estimation Method

The initial condition estimation technique has been proposed in [15] to estimate a spatiotemporal chaotic signal $\mathbf{x}_n$ generated by $\mathbf{h}$ in additive random noise $\mathbf{w}_n$. Let $\mathbf{y}_n$ be its noisy observation, that is

$$\mathbf{y}_n = \mathbf{x}_n + \mathbf{w}_n, \tag{1}$$

$$\mathbf{x}_n = \mathbf{h}(\mathbf{x}_{n-1}),\ n = 0, 1, \cdots, N-1 \tag{2}$$

where $\mathbf{y}_n = [y_n^1\ y_n^2\ \cdots\ y_n^M]^T$, $\mathbf{x}_n = [x_n^1\ x_n^2\ \cdots\ x_n^M]^T$ and $\mathbf{w}_n = [w_n^1\ w_n^2\ \cdots\ w_n^M]^T$. Here, M is the number of channels and N is the sequence length. The spatiotemporal chaotic map $\mathbf{h}$ is the nonlinear and noninvertible map which is modeled by a CML system. If the initial condition, namely, $\mathbf{x}_0$, is perfectly estimated from $\{\mathbf{y}_n\}_0^{N-1}$, the noise-free $\{\mathbf{x}_n\}_0^{N-1}$ can be obtained according to (2), where $\{\mathbf{a}_n\}_0^{N-1}$ represents $\{\mathbf{a}_n | n = 0, 1, \cdots, N-1\}$.

Considering the typical diffusive CML [10] with M sites labeled m , x_n^m is modeled as

$$x_{n+1}^m = (1-\epsilon) f(x_n^m) + \epsilon/2 \left[f(x_n^{m-1}) + f(x_n^{m+1}) \right],\ m = 1, 2, \cdots, M \tag{3}$$

along with rules for periodic boundary condition, that is, when $m = 1$ and $m = M$, we have $x_{n+1}^1 = (1-\epsilon) f(x_n^1) + \epsilon/2[f(x_n^M) + f(x_n^2)]$ and $x_{n+1}^M = (1-\epsilon) f(x_n^M) + \epsilon/2[f(x_n^{M-1}) + f(x_n^1)]$, respectively. The ϵ denotes the coupling coefficient and f is the chaotic map. The vector form of (3) is

$$\mathbf{x}_{n+1} = \mathbf{h}(\mathbf{x}_n) = \mathbf{A}\mathbf{f}(\mathbf{x}_n) \tag{4}$$

where $\mathbf{f}(\mathbf{x}_n) = \left[f(x_n^1)\ f(x_n^2)\ \cdots\ f(x_n^M) \right]^T$ and $\mathbf{A}$ is the $M \times M$ Toeplitz coupling matrix with the first column $\mathbf{a}$ and the first row $\mathbf{a}^T$, $\mathbf{a} = [1-\epsilon\ \epsilon/2\ \underbrace{0\ \cdots\ 0}_{M-3}\ \epsilon/2]^T$.

Here we assume that the coupling coefficient ϵ and dynamics of the local map f are known. Since f is a nonlinear and many-to-one function, its inverse function does not exist within its whole phase space. Therefore, the symbolic dynamic, which is a coarse-grained description of dynamics [14], [18], has been introduced to make f invertible within one partition of the phase space. The idea of symbolic dynamics is that we firstly divide the phase space into a finite number of partitions and label each partition by a number. Here, the map f in each partition is monotonic. Then we record the alternation of the numbers instead of the accurate values of the signal points. In this paper, we focus on the maps that their symbolic dynamics are completely developed. Let $\mathbb{P}^m = \{P_0^m, P_1^m, ..., P_{q-1}^m\}$ be a finite disjoint partition of the mth phase space in the CML system, that is, $\bigcup_{k=0}^{q-1} P_k^m = I$, $P_k^m \bigcap P_l^m = \phi$ for $k \neq l$. We assume that at time n, the phase point x_n^m lies in the kth element of the partition P_k^m, and we assign a symbol $s_n^m = k$, where $k \in \{0, 1, \ldots, q-1\}$. If the ergodicity is preserved by the coupling, that is, the behavior of a dynamical system averaged over time is the same as averaged over space, then any orbit in phase space I^M of the CML system can be encoded as a semi-infinite symbolic vector sequence $\{\mathbf{s}_0, \mathbf{s}_1, \ldots, \mathbf{s}_n, \ldots\}$ where $\mathbf{s}_n = [s_n^1 \; s_n^2 \; \cdots \; s_n^M]^T$ [14].

When $\mathbf{A}$ is nonsingular, we get $\mathbf{f}(\mathbf{x}_n) = \mathbf{A}^{-1}\mathbf{x}_{n+1}$, where $\mathbf{A}^{-1}$ is the inverse matrix of $\mathbf{A}$. With the introduction of the symbolic vector $\mathbf{s}_n$, the maps $\mathbf{f}$ are monotonic functions in each disjoint partition. The inverse function of CML [8], [14] can then be generalized as

$$\mathbf{x}_n = \mathbf{h}_{\mathbf{s}_n}^{-1}(\mathbf{x}_{n+1}) = \mathbf{f}_{\mathbf{s}_n}^{-1}\left(\mathbf{A}^{-1}\mathbf{x}_{n+1}\right) \tag{5}$$

where $\mathbf{h}_{\mathbf{s}_n}^{-1} = \mathbf{f}_{\mathbf{s}_n}^{-1} \circ \mathbf{A}^{-1}$, $\mathbf{f}_{\mathbf{s}_n}^{-1}(\mathbf{x}_n) = [f_{s_n^1}^{-1}(x_n^1) \; f_{s_n^2}^{-1}(x_n^2) \; \cdots \; f_{s_n^M}^{-1}(x_n^M)]^T$ and $\circ$ denotes the composition operator. In fact, we use $\mathbf{y}_{n+1}$ instead of $\mathbf{x}_{n+1}$ in (5) since $\mathbf{x}_{n+1}$ is unknown. It is well known that some tiny errors will generate large errors via iterations when the system diverges. Therefore, we need to investigate the convergence and divergence properties of inverse CML systems with different maps and coupling coefficients to evaluate that the estimated initial condition is effective or not.

It is proved [8] that when the inverse function of CML $\mathbf{h}_{\mathbf{s}_n}^{-1}$ is the contraction map and the symbolic vector sequence $\{\mathbf{s}_n\}_0^{N-1}$ is known, then we have

$$\lim_{N \to \infty} \mathbf{h}_{\{\mathbf{s}_n\}_0^{N-1}}^{-(N-1)}(\boldsymbol{\eta}) = \mathbf{x}_0 \tag{6}$$

where $\mathbf{h}_{\{\mathbf{s}_n\}_0^{N-1}}^{-(N-1)}(\boldsymbol{\eta}) = \mathbf{h}_{\mathbf{s}_0}^{-1}\left(\mathbf{h}_{\mathbf{s}_1}^{-1} \cdots \mathbf{h}_{\mathbf{s}_{N-1}}^{-1}(\boldsymbol{\eta})\right)$ and $\boldsymbol{\eta}$ is randomly selected within the phase space I^M.

However, the contraction mapping theorem only provides a sufficient condition for convergence. In this paper, we focus on finding a sufficient and necessary condition for convergence.

III. The Convergence Properties

A. Largest Lyapunov Exponent

Lyapunov exponent (LE), which gives the rate of exponential separation or convergence of two infinitesimally close initial conditions in phase space, is a very important character in the spatially extended system [19]. For CML systems, since its dimension is larger than one, there exists a set of

Lyapunov exponents called Lyapunov spectrum, in which the largest of them is the most important character to describe the development of a small deviation [20], [21]. For time series produced by dynamical systems, the presence of a positive LE indicates orbital divergence and chaos, while a negative or zero-valued LE is a characteristic for regular behavior. Therefore, the largest LE in an inverse CML system, which is referred to as the ILLE, is utilized to study the convergence and divergence properties for the inverse CML systems.

It is well known that if λ is the largest LE of a deterministic map : $\mathbf{z}_{n+1} = \mathbf{g}(\mathbf{z}_n)$, where $\mathbf{z}, \mathbf{g} \in \mathbb{R}^K$, $n = 0, 1, \cdots$ and $\mathbb{R}^K$ denotes the set of K-dimensional real vector, we have [20], [21]

$$\|\mathbf{g}^n(\mathbf{z}_0) - \mathbf{g}^n(\mathbf{z}_0 + \boldsymbol{\xi})\|_2 \approx \|\boldsymbol{\xi}\|_2 \exp(\lambda n) \tag{7}$$

where $\boldsymbol{\xi}$ is the uncertainty in the initial condition. In the inverse CML system of (5), the ILLE, denoted by $\beta_{\max}(f, \epsilon)$, approximately satisfies the following equation

$$\left\|\mathbf{x}_0 - \widehat{\mathbf{x}}_{0|N-1}\right\|_2 = \|\delta(\mathbf{x}_{(N-1)})\|_2 \exp\left(\beta_{\max}(f, \epsilon)(N-1)\right) \tag{8}$$

where $\|\delta(\mathbf{x}_{N-1})\|_2$ is the uncertainty in $\mathbf{x}_{N-1}$ and $\widehat{\mathbf{x}}_{0|N-1}$ denotes the estimated value of $\mathbf{x}_0$ with $(N-1)$ iterative steps.

Dividing (8) by $\|\delta(\mathbf{x}_{N-1})\|_2$ and taking the limit as $\|\delta(\mathbf{x}_{N-1})\|_2 \to 0$ gives

$$\exp\left(\beta_{\max}(f, \epsilon)(N-1)\right) = \|\mathbf{J}_{\mathbf{h}^{-(N-1)}_{\{\mathbf{s}_n\}_0^{N-1}}(\mathbf{x}_{N-1})}\|_2 \tag{9}$$

where $\mathbf{J}_{\mathbf{h}^{-(N-1)}_{\{\mathbf{s}_n\}_0^{N-1}}(\mathbf{x}_{N-1})}$ is the Jacobian matrix of function $\mathbf{x}_0 = \mathbf{h}^{-(N-1)}_{\{\mathbf{s}_n\}_0^{N-1}}(\mathbf{x}_{N-1})$. That is

$$\mathbf{J}_{\mathbf{h}^{-(N-1)}_{\{\mathbf{s}_n\}_0^{N-1}}(\mathbf{x}_{N-1})} = \frac{\partial \mathbf{x}_0}{\partial \mathbf{x}_{N-1}^T} = \frac{\partial \mathbf{x}_0}{\partial \mathbf{x}_1^T}\frac{\partial \mathbf{x}_1}{\partial \mathbf{x}_2^T} \cdots \frac{\partial \mathbf{x}_{N-2}}{\partial \mathbf{x}_{N-1}^T} = \prod_{n=0}^{N-2} \mathbf{J}_{\mathbf{f}^{-1}_{\mathbf{s}_n}(\bar{\mathbf{x}}_{n+1})} \mathbf{A}^{-1} \tag{10}$$

where $\bar{\mathbf{x}}_n = \mathbf{A}^{-1}\mathbf{x}_n$ and $\mathbf{J}_{\mathbf{f}^{-1}_{\mathbf{s}_n}(\bar{\mathbf{x}}_{n+1})}$ is the Jacobian matrix of inverse chaotic map $\mathbf{f}^{-1}_{\mathbf{s}_n}(\bar{\mathbf{x}}_{n+1})$.

Noting that the spectral radius of a symmetric matrix $\mathbf{J}_{\mathbf{h}^{-(N-1)}_{\{\mathbf{s}_n\}_0^{N-1}}(\mathbf{x}_{N-1})}$, denoted by ρ, is equal to its matrix 2-norm and taking the limit $N \to \infty$ on the both sides of (9), we obtain

$$\beta_{\max}(f, \epsilon) = \lim_{N\to\infty} \frac{1}{N-1} \ln(\rho) = \lim_{N\to\infty} \frac{1}{N-1} \ln\left(\max_{1\le m\le M}(|r_m|)\right) \tag{11}$$

where $r_1, \cdots, r_M$ are the eigenvalues of the matrix $\mathbf{J}_{\mathbf{h}^{-(N-1)}_{\{\mathbf{s}_n\}_0^{N-1}}(\mathbf{x}_{N-1})}$. Hence the ILLE can be determined when the map and coupling coefficient are known.

Since a positive largest LE indicates chaos, and a negative largest LE indicates temporal periodic behavior and spatially invariant structure with time [19], we have the following lemma.

Lemma. *Given a CML system with a known map and coupling coefficient, and if $\{\mathbf{s}_n\}$ is correct, the initial condition can be perfectly obtained as*

$$\lim_{N\to\infty} \widehat{\mathbf{x}}_{0|(N-1)} = \lim_{N\to\infty} \mathbf{h}^{-(N-1)}_{\{\mathbf{s}_n\}_0^{N-1}}(\boldsymbol{\eta}) = \mathbf{x}_0 \tag{12}$$

if and only if the ILLE of the CML system is negative for arbitrary $\boldsymbol{\eta} \in I^M$. In addition, the convergence rate of the backward iterative approximation error is exponentially proportional to the ILLE according to (8). Otherwise, we cannot estimate the initial condition in the CML systems.

Proof: According to (8), $\left\|\mathbf{x}_0 - \widehat{\mathbf{x}}_{0|N-1}\right\|_2 = \|\delta(\mathbf{x}_{(N-1)})\|_2 \exp\left(\beta_{\max}(f,\epsilon)(N-1)\right)$, take the limit $(N-1) \to \infty$ on both sides, we have $\lim_{N\to\infty} \widehat{\mathbf{x}}_{0|(N-1)} = \mathbf{x}_0$ when the ILLE of the CML system, $\beta_{\max}(f,\epsilon)$, is negative. ∎

B. Examples

In order to show the calculations of the inverse function $\mathbf{h}_{\mathbf{s}_n}^{-1}$ and Jacobian matrix $\mathbf{J}_{\mathbf{f}_{\mathbf{s}_n}^{-1}(\bar{\mathbf{x}}_{n+1})}$, without loss of generality, we use the CML systems with logistic map (CML-logistic) and tent map (CML-tent) as illustrations. Their vector forms, denoted by $\mathbf{f}_L(\mathbf{x}_n)$ and $\mathbf{f}_T(\mathbf{x}_n)$, respectively, are

$$\mathbf{f}_L(\mathbf{x}_n) = \boldsymbol{\mu}_L . * \mathbf{x}_n . * (\mathbf{1}_{M\times 1} - \mathbf{x}_n) \tag{13}$$

$$\mathbf{f}_T(\mathbf{x}_n) = \boldsymbol{\mu}_T . * (\mathbf{1}_{M\times 1} - 2|\mathbf{x}_n - 0.5\mathbf{1}_{M\times 1}|) \tag{14}$$

where $\mathbf{a}. * \mathbf{b}$ is the element-wise multiplication of $\mathbf{a}$ by $\mathbf{b}$ and $\mathbf{1}_{M\times 1}$ denotes the $M \times 1$ vector with all elements 1. The $\boldsymbol{\mu}_L = [\mu_L^1\, \mu_L^2\, \cdots \mu_L^M]^T$ and $\boldsymbol{\mu}_T = [\mu_T^1\, \mu_T^2\, \cdots \mu_T^M]^T$ are the parameters that dramatically affect the behavior of the map.

The inverse functions of CML-logistic and CML-tent systems, denoted by $\mathbf{h}_{L,\mathbf{s_n}}^{-1}$ and $\mathbf{h}_{T,\mathbf{s_n}}^{-1}$, respectively, are

$$\mathbf{x}_n = \mathbf{h}_{L,\mathbf{s_n}}^{-1}(\mathbf{x}_{n+1}) = \mathbf{f}_{L,\mathbf{s}_n}^{-1}(\mathbf{A}^{-1}\mathbf{x}_{n+1}) = 0.5\mathbf{1}_{M\times 1} + 0.5(2\mathbf{s}_n - \mathbf{1}_{M\times 1}). * \sqrt{\mathbf{1}_{M\times 1} - 4\bar{\mathbf{x}}_{n+1}./\boldsymbol{\mu}_L} \tag{15}$$

$$\mathbf{x}_n = \mathbf{h}_{T,\mathbf{s_n}}^{-1}(\mathbf{x}_{n+1}) = \mathbf{f}_{T,\mathbf{s}_n}^{-1}(\mathbf{A}^{-1}\mathbf{x}_{n+1}) = 0.5\mathbf{1}_{M\times 1} + 0.5(2\mathbf{s}_n - \mathbf{1}_{M\times 1}). * (\mathbf{1}_{M\times 1} - \bar{\mathbf{x}}_{n+1}./\boldsymbol{\mu}_T) \tag{16}$$

where $\mathbf{a}./\mathbf{b}$ represents element-wise division of $\mathbf{a}$ by $\mathbf{b}$, $\sqrt{\mathbf{a}}$ is the element-wise square root of $\mathbf{a}$, and

$$s_n^m = \begin{cases} 0, & x_n^m < 0.5 \\ 1, & x_n^m \geq 0.5. \end{cases} \tag{17}$$

The Jacobian matrix of the inverse logistic map $\mathbf{f}_{L,\mathbf{s}_n}^{-1}(\bar{\mathbf{x}}_{n+1})$ and that of the inverse tent map $\mathbf{f}_{T,\mathbf{s}_n}^{-1}(\bar{\mathbf{x}}_{n+1})$, denoted by $\mathbf{J}_{\mathbf{f}_{L,\mathbf{s}_n}^{-1}(\bar{\mathbf{x}}_{n+1})}$ and $\mathbf{J}_{\mathbf{f}_{T,\mathbf{s}_n}^{-1}(\bar{\mathbf{x}}_{n+1})}$, respectively, are

$$\mathbf{J}_{\mathbf{f}_{L,\mathbf{s}_n}^{-1}(\bar{\mathbf{x}}_{n+1})} = \mathrm{diag}\left(-\left(2\mathbf{s}_n - \mathbf{1}_{M\times 1}\right)./\left(\boldsymbol{\mu}_L . * \sqrt{\mathbf{1}_{M\times 1} - 4\bar{\mathbf{x}}_{n+1}/\boldsymbol{\mu}_L}\right)\right) \tag{18}$$

$$\mathbf{J}_{\mathbf{f}_{T,\mathbf{s}_n}^{-1}(\bar{\mathbf{x}}_{n+1})} = \mathrm{diag}\left(-0.5\left(2\mathbf{s}_n - \mathbf{1}_{M\times 1}\right)./\boldsymbol{\mu}_T\right) \tag{19}$$

where diag represents the diagonal operator. According to (10) and (11), the ILLEs for the CML-logistic and CML-tent systems are obtained.

IV. Cramér-Rao Lower Bound

The CRLB gives a lower bound on variance attainable by any unbiased estimators using the same data, and thus it can be served as an important benchmark to compare with the mean square error (MSE) of the initial condition estimation method. Therefore, in this section, the CRLB based on the model of (1) subject to (4) is derived. For simplicity but without loss of generality, here we assume uncorrelated zero-mean Gaussian noise with variance $\{\sigma_m^2\}$. Our task is to estimate $\mathbf{x}_0$ from $\{\mathbf{y}_n\}_0^{N-1}$. We first have [22]:

$$\mathbf{y}_n \sim \mathcal{N}\left(\mathbf{A}\mathbf{f}(\mathbf{x}_{n-1}), \mathbf{C}\right) \tag{20}$$

That is, $\mathbf{y}_n$ is Gaussian distributed with mean $\mathbf{A}\mathbf{f}(\mathbf{x}_{n-1})$ and covariance $\mathbf{C} = \mathrm{diag}(\left[\sigma_1^2\ \sigma_2^2\ \cdots\ \sigma_M^2\right])$. Its probability density function (PDF) is

$$p\left(\{\mathbf{y}_n\}_0^{N-1}; \mathbf{x}_0\right) = \frac{1}{(2\pi)^{N/2}\mathrm{det}^{1/2}[\mathbf{C}]}\exp\left[-\frac{1}{2}\sum_{n=0}^{N-1}\left(\mathbf{y}_n - \mathbf{x}_n\right)^T\mathbf{C}^{-1}\left(\mathbf{y}_n - \mathbf{x}_n\right)\right] \tag{21}$$

where det represents matrix determinant.

The Fisher information matrix (FIM) for $\mathbf{x}_0$ estimated from $\{\mathbf{y}_n\}_0^{N-1}$, denoted by $\mathrm{FIM}(\mathbf{x}_{0|N-1})$, is

$$\mathrm{FIM}(\mathbf{x}_{0|N-1}) = \sum_{n=0}^{N-1}\mathbf{B}_n^T\mathbf{C}^{-1}\mathbf{B}_n \tag{22}$$

where

$$\mathbf{B}_n = \frac{\partial \mathbf{x}_n}{\partial \mathbf{x}_0^T} = \begin{cases}\mathbf{I}_{M\times M}, & \text{if } n = 0\\ \prod_{i=n-1}^{0}\mathbf{A}\mathbf{J}_{\mathbf{f}(\mathbf{x}_i)}, & \text{if } n > 0\end{cases}$$

with $\mathbf{I}_{M\times M}$ being the $M\times M$ identity matrix. The $\mathbf{J}_{\mathbf{f}(\mathbf{x}_n)}$ is the Jacobian matrix of chaotic map $\mathbf{f}(\mathbf{x}_n)$, which has the form

$$\mathbf{J}_{\mathbf{f}(\mathbf{x}_n)} = \frac{\partial \mathbf{f}(\mathbf{x}_n)}{\partial \mathbf{x}_n^T} = \mathrm{diag}\left([f'(x_n^1)\ f'(x_n^2)\cdots\ f'(x_n^M)]^T\right) \tag{23}$$

where $f'(x_n^m)$ denotes the derivative of $f(x_n^m)$. For example, the Jacobian matrix of logistic map $\mathbf{f}_L(\mathbf{x}_n)$ and tent map $\mathbf{f}_T(\mathbf{x}_n)$, denoted by $\mathbf{J}_{\mathbf{f}_L(\mathbf{x}_n)}$ and $\mathbf{J}_{\mathbf{f}_T(\mathbf{x}_n)}$, respectively, are

$$\mathbf{J}_{\mathbf{f}_L(\mathbf{x}_n)} = \frac{\partial \mathbf{f}_L(\mathbf{x}_n)}{\partial \mathbf{x}_n^T} = \mathrm{diag}\left(2\boldsymbol{\mu}_L.*\left(\mathbf{1}_{M\times 1} - 2\mathbf{x}_n\right)\right) \tag{24}$$

$$\mathbf{J}_{\mathbf{f}_T(\mathbf{x}_n)} = \frac{\partial \mathbf{f}_T(\mathbf{x}_n)}{\partial \mathbf{x}_n^T} = \mathrm{diag}\left(-2\boldsymbol{\mu}_T.*\left(2\mathbf{s}_n - \mathbf{1}_{M\times 1}\right).*\mathbf{x}_n\right) \tag{25}$$

Since the diagonal elements of the FIM inverse are the minimum achievable variance values, the CRLB of x_0^m estimated from $\{\mathbf{y}\}_0^{N-1}$, denoted by $\mathrm{CRLB}(x_{0|N-1}^m)$, is

$$\mathrm{CRLB}(x_{0|N-1}^m) = \left[\left(\mathrm{FIM}(\mathbf{x}_{0|N-1})\right)^{-1}\right]_{m,m} \tag{26}$$

where $[\mathbf{A}]_{m,m}$ is the (m,m) entry of $\mathbf{A}$.

V. SIMULATION RESULTS

Simulation results are carried out to confirm the effectiveness of the CML initial condition estimation method of (5) in CML-logistic and CML-tent systems with different system parameters. Here, the number of lattices is $M = 5$ and initial condition is $\mathbf{x}_0 = [0.2\ 0.4\ 0.6\ 0.8\ 0.9]^T$. Moreover, the CML-logistic and CML-tent systems are with identical map parameters of $\mu_L^m = \mu_L$ and $\mu_T^m = \mu_T$, respectively.

A. ILLE in CML systems

The ILLEs of the CML-logistic and CML-tent systems are plotted in Figs. 1 (a) and (b), respectively. The coupling coefficient for both maps varies from 0 to 0.5, $\mu_L \in [3.57\ 4]$ and $\mu_T \in [0.5\ 1]$. The black area corresponds to a negative ILLE while the gray area represents the positive ILLE. We observe that the ILLEs for the CML-tent system are smoother than those for the CML-logistic system, because the chaotic characteristics between logistic map and tent map are different. That is, the logistic map experiences a more complex procedure which includes chaotic and oscillation alternately when μ_L varies from 3.57 to 4, while the tent map transits from regular to chaotic when μ_T varies from 0.5 to 1. Furthermore, the area of negative ILLE for the CML-tent system is larger than that for CML-logistic system, which means that the initial condition estimation method can be applied more widely in CML-tent system. For example, when $\epsilon = 0.2$, $\mu_L = 4$ and $\mu_T = 1$, the ILLE for CML-tent system is negative while that for CML-logistic system is positive.

B. Initial condition estimation in CML systems

The estimation performance is evaluated by MSE. Here, the MSE for each backward iterative step i, denoted by $\mathrm{MSE}(i)$, is defined as

$$\mathrm{MSE}(i) = \frac{1}{L}\sum_{j=1}^{L} \|\mathbf{x}_{N-1-i} - \widehat{\mathbf{x}}_{N-1-i}^{(j)}\|_2^2,\ i = 0, 1, \cdots, N-1 \tag{27}$$

where L is the number of independent runs, and $\widehat{\mathbf{x}}_n^{(j)}$ is the estimated value of $\mathbf{x}_n$ in the jth independent run. The MSE, convergence rate (CR), and CRLB in dB are defined as follows:

$$\mathrm{MSE}(i)_{\text{dB}} = 10\log_{10}(\mathrm{MSE}(i)) \tag{28}$$

$$\mathrm{CR}(i)_{\text{dB}} \approx 20\log_{10}\left(\|\delta(\mathbf{x}_{N-1})\|_2 \exp\left(\beta_{\max}(f, \epsilon) i\right)\right) \tag{29}$$

$$\mathrm{CRLB}(\mathbf{x}_{0|N-1})_{\text{dB}} = 10\log_{10}\left(\sum_{m=1}^{M} \mathrm{CRLB}(x_{0|N-1}^m)\right) \tag{30}$$

where the CR which exposes the convergence rate of two close points when $\beta_{\max}(f, \epsilon) < 0$ is just the approximation form according to (8). All simulation results are averages of $L = 500$ independent runs.

Firstly, the effectiveness of the initial condition estimation method in CML-logistic system with $\mu_L = 4$ is tested with the correct symbolic vector sequence and the results are plotted in Fig. 2. In each independent run, we randomly select $\boldsymbol{\eta}$ within the phase space I^M as the estimated value of the $(N-1)$th time step. According to Fig. 2 (a), the MSEs roughly align with its corresponding CR curve when $\epsilon = 0.01, 0.05, 0.1$, here $\|\delta(\mathbf{x}_{N-1})\|_2 = \sqrt{M}\|\boldsymbol{\eta} - \mathbf{x}_{N-1}\|_2$. In fact, in these cases, their corresponding systems are all with negative ILLEs which illustrate the effectiveness of the initial condition estimation method. The CML-logistic systems with $\epsilon = 0.01$ and $\epsilon = 0.1$ reach the floating point relative accuracy in MATLAB around $i = 60$ and $i = 120$, respectively, which indicate that (i) the estimated result achieves the real value that represented by (12), and (ii) the smaller the negative ILLE is, the faster the convergence rate is. On the other hand, the MSEs with $\epsilon = 0.35,\ 0.4$ are very large and cannot converge to the real value since their corresponding ILLEs are positive as shown in Fig. 2 (b).

Secondly, the above test is repeated in CML-tent system with $\mu_T = 1$. As seen in Fig. 3 (a), the MSEs for CML-tent system align quite well with their corresponding CR curves because the inverse CML-tent system is a contraction map in these cases, while the inverse CML-logistic system is not [16], [17]. Furthermore, the MSEs diverge when the ILLE is larger than zero as described in Fig. 3 (b).

Finally, the signal estimation from noisy measurements $\{\mathbf{y}_n\}_0^{N-1}$ is investigated. Here, we consider the signal model of (1) subject to (4) with logistic map of (13) and tent map of (14), and investigate three types of noises $\{\mathbf{w}_n\}_0^{N-1}$, namely, Gaussian, exponential and Rayleigh noises, respectively. All noises are assigned same variance of $\sigma_i^2 = \sigma^2$ and their mean values are 0, σ and $\sqrt{(\pi\sigma^2)/(4-\pi)}$, respectively. The estimated symbolic vector sequence $\{\widehat{\mathbf{s}}_n\}_0^{N-1}$ is obtained using $\{\mathbf{y}_n\}_0^{N-1}$, that is, $\hat{s}_n^m = \begin{cases} 0, & y_n^m < 0.5 \\ 1, & y_n^m \geq 0.5 \end{cases}$. The sequence length is $N = 10$, and the MSEs with $(N-1)$ iterative steps, denoted by MSE$(N-1)_{\mathrm{dB}}$, versus different noise power σ^2 when $\epsilon = 0.1$ and $\epsilon = 0.4$ are shown in Figs. 4 and 5, respectively. The MSEs for CML-logistic and CML-tent systems with Gaussian noises can approach CRLB at $\sigma^2 \leq -35$dB and $\sigma^2 \leq -55$dB when $\epsilon = 0.1$ as can be seen in Figs. 4 (a) and (b), respectively, while they both cannot attain CRLB when $\epsilon = 0.4$ with the same initial condition estimation method as shown in Fig. 5. Furthermore, the performance under these three noise distributions is comparable, that is, the estimation method works properly in Gaussian and non-Gaussian noises when the ILLE is negative. It is worth noting that the estimation method does not require the values of noise variance and mean.

VI. Conclusion

In this paper, the effectiveness of initial condition estimation method for coupled map lattice (CML) systems with different coupled coefficients and maps are fully investigated based on the convergence and divergence properties of their inverse systems. The reason which leads to invalid estimation is investigated and the inverse largest Lyapunov exponent (ILLE) for CML systems, is utilized to determine the effectiveness of the CML initial condition estimation method. Theoretical and experimental results show that the CML initial condition estimation method is effective if and only if the ILLE is negative. Otherwise, it is an invalid estimation method.

ACKNOWLEDGEMENT

This work was partly supported by the Natural Science Foundation of China (No. 61072037) and Natural Science Foundation of Guangdong.

REFERENCES

[1] G. W. Frank, T. Lookman, M. A. H. Nerenberg, C. Essex, J. Lemieux, and W. Blume, "Chaotic time series analyses of epileptic seizures," *Physica D: Nonlinear Phenomena*, vol. 46, no. 3, pp. 427–438, 1990.

[2] G. P. Williams, *Chaos Theory Tamed*. Joseph Henry Press, 1997.

[3] S. Kay and V. Nagesha, "Methods for chaotic signal estimation," *IEEE Transactions on Signal Processing*, vol. 43, no. 8, pp. 2013–2016, 1995.

[4] H. C. Papadopoulos and G. W. Wornell, "Maximum-likelihood estimation of a class of chaotic signals," *IEEE Transactions on Information Theory*, vol. 41, no. 1, pp. 312–317, Jan. 1995.

[5] S. Kay, "Asymptotic maximum likelihood estimator performance for chaotic signals in noise," *IEEE Transactions on Signal Processing*, vol. 43, no. 4, pp. 1009–1012, April 1995.

[6] V. M. Alekseev and M. V. Yakobson, "Symbolic dynamics and hyperbolic dynamic systems," *Physics Reports*, vol. 75, no. 5, pp. 287–325, 1981.

[7] C. Ling, X. F. Wu, and S. G. Sun, "A general efficient method for chaotic signal estimation," *IEEE Transactions on Signal Processing*, vol. 47, no. 5, pp. 1424–1428, May 1999.

[8] K. Wang, W. J. Pei, S. P. Wang, Y. M. Cheung, and Z. Y. He, "Symbolic vector dynamics approach to initial condition and control parameters estimation of coupled map lattices," *IEEE Transactions on Circuits Systems I: Regular Papers*, vol. 55, no. 4, pp. 1116–1124, May 2008.

[9] D. Coca and S. A. Billings, "Identification of coupled map lattice models of complex spatio-temporal patterns," *Physics Letters A*, pp. 65–73, Aug. 2001, 287.

[10] K. Kaneko, "Spatio-temporal intermittency in coupled map lattices," *Progress of Theoretical Physics*, vol. 74, pp. 1033–1044, 1985.

[11] H. Leung, G. Hennessey, and A. Drosopoulos, "Signal detection using the radial basis function coupled map lattice," *IEEE Transactions on Neural Networks*, vol. 11, no. 5, Sept. 2000.

[12] Y. C. Zeng and Q. Y. Tong, "A statistical property to recover coarsely initial conditions from coupled map lattices," *Acta Physica Sinica*, vol. 52, pp. 285–291, 2003.

[13] Y. Liu, M. F. Shen, and H. Y. Chen, "Recovery of statistical property of initial conditions based on time-varying parameter from coupled map lattices," *Acta Physica Sinica*, pp. 564–571, 2006.

[14] S. D. Pethel, N. J. Corron, and E. Bollt, "Symbolic dynamics of coupled map lattices," *Physical Review Letters*, vol. 96, 2006, 034105.

[15] K. Wang, W. J. Pei, Z. Y. He, and Y. M. Cheung, "Estimating initial conditions in coupled map lattices from noisy time series using symbolic vector dynamics," *Physics Letters A*, vol. 367, no. 4-5, pp. 316–321, 2007.

[16] M. F. Shen, L. X. Lin, X. Y. Li, and C. Q. Chang, "Initial condition estimate from coupled map lattices system based on symbolic dynamics," *Acta Physica Sinica*, vol. 58, pp. 47–55, 2009.

[17] L. S. Sun, X. Y. Kang, and L. X. Lin, "Analysis of convergence for initial condition estimation of coupled map lattices based on symbolic dynamics," *Chinese Physics B*, vol. 19, no. 11, 2010, 110507.

[18] B.-L. Hao, "Applied symbolic dynamics," *Chinese Journal of Physics*, vol. 36, no. 6, pp. 753–757, 1998.

[19] K. Kaneko, "Lyapunov analysis and information flow in coupled map lattices," *Physica D*, vol. 23, pp. 436–447, 1986.

[20] J. P. Eckmann and D. Ruelle, "Ergodic theory of chaos and strange attractors," *Reviews of Modern Physics*, vol. 57, no. 3, pp. 617–656, July 1985.

[21] M. T. Rosenstein, J. J. Collins, and C. J. De Luca, "A practical method for calculating largest Lyapunov exponents from small data sets," *Physica D*, vol. 65, pp. 117–134, 1993.

[22] S. M. Kay, *Fundamentals of Statistical Signal Processing: Estimation Theory*. Englewood Cliffs, NJ: Prentice-Hall, 1993.

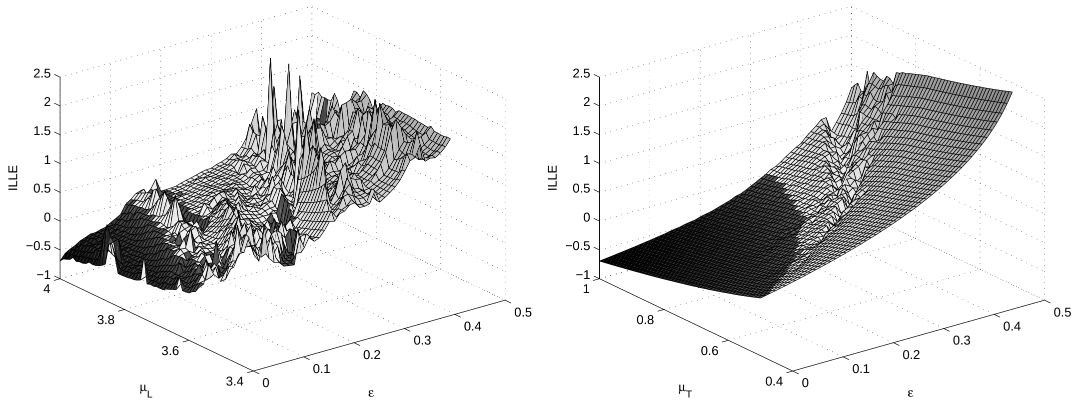

(a) (b)

Fig. 1. ILLE in CML system with different system parameters; (a) CML-logistic system with $\mu_L \in [3.57\ 4]$, $\epsilon \in [0\ 0.5]$; (b) CML-tent system with $\mu_T \in [0.5\ 1]$, $\epsilon \in [0\ 0.5]$.

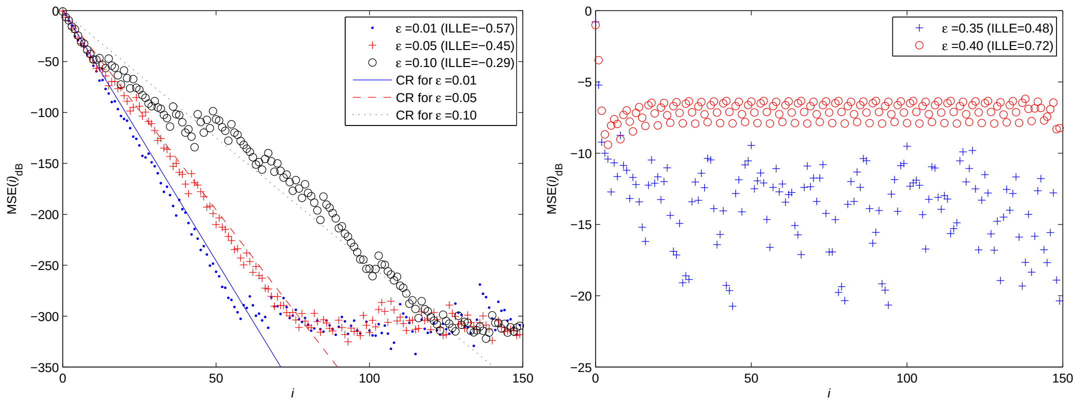

(a) (b)

Fig. 2. MSE versus iterative step with difference ϵ in CML-logistic system when $\mu_L = 4$; (a) $\epsilon = 0.01,\ 0.05,\ 0.1$; (b) $\epsilon = 0.35,\ 0.4$.

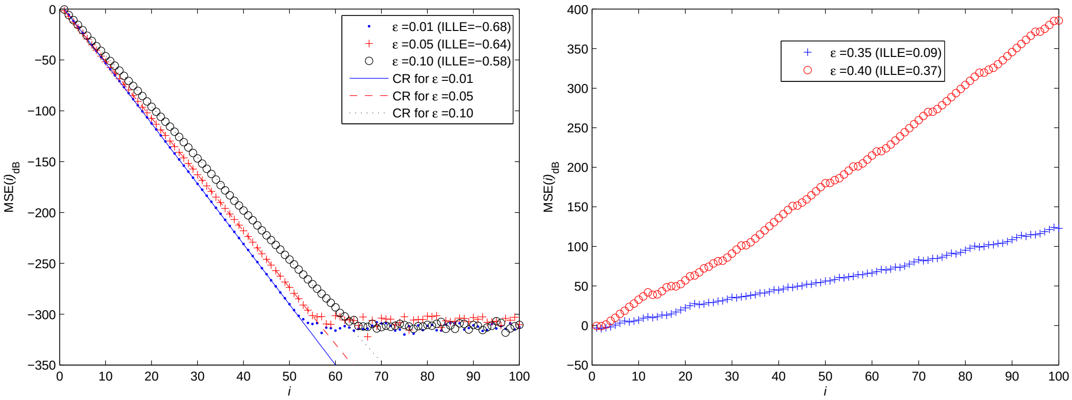

(a) (b)

Fig. 3. MSE versus iterative step with difference ϵ in CML-tent system when $\mu_T = 1$; (a) $\epsilon = 0.01, 0.05, 0.1$; (b) $\epsilon = 0.35, 0.4$.

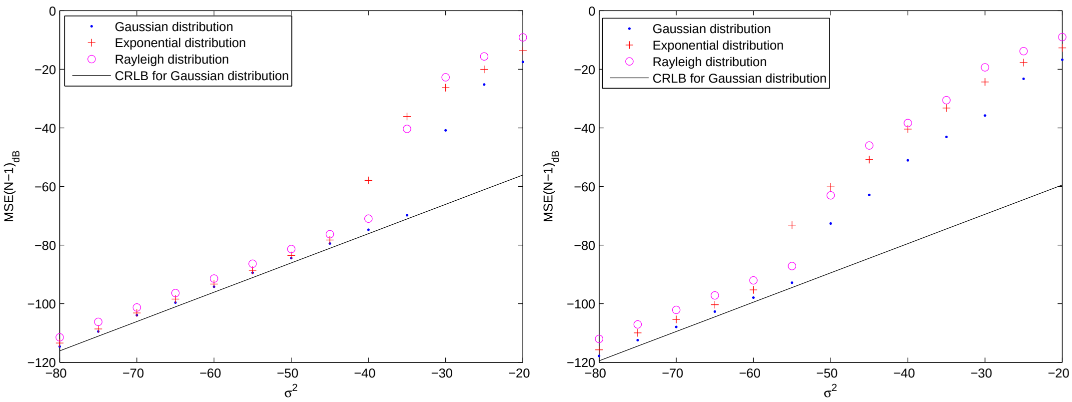

(a) (b)

Fig. 4. MSE versus σ^2 with $\epsilon = 0.1$, $N = 10$ when the noises follow Gaussian, exponential and Rayleigh distribution, respectively; (a) CML-logistic system; (b) CML-tent system.

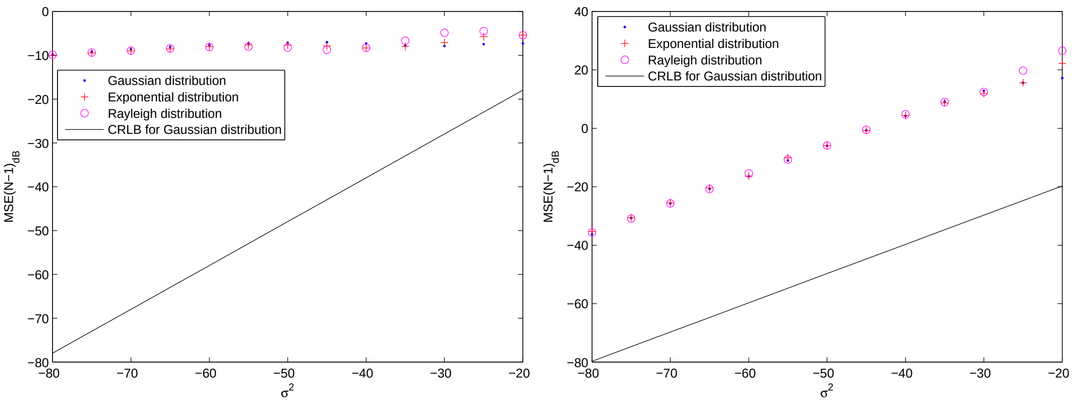

(a) (b)

Fig. 5. MSE versus σ^2 with $\epsilon = 0.4$, $N = 10$ when the noises follow Gaussian, exponential and Rayleigh distribution, respectively; (a) CML-logistic system; (b) CML-tent system.